ACTA MECHANICA SINICA (English Series), Vol.12, No.4, Nov. 1996 ISSN 0567-7718
The Chinese Society of Theoretical and Applied Mechanics
Chinese Journal of Mechanics Press, Beijing, China
Allerton Press, INC., New York, U.S.A.

A NEW N-BODY POTENTIAL AND ITS APPLICATION

Tang Qiheng (汤奇恒) Wang Tzuchiang (王自强) Zhang Yongwei (张永伟)
(*Institute of Mechanics, Chinese Academy of Sciences, Beijing* 100080, *China*)

ABSTRACT: Based on the embedded atom method (EAM) proposed by Daw and Baskes and Johnson's model, this paper constructs a new N-body potential for bcc crystal Mo. The procedure of constructing the new N-body potential can be applied to other metals. The dislocation emission from a crack tip has been simulated successfully using molecular dynamics method, the result is in good agreement with the elastic solution.

KEY WORDS: embedded atom method (EAM), N-body potential, dislocation emission, molecular dynamics

1 INTRODUCTION

The material behavior is an important subject of mechanics, materials science and solid state physics. The strength of materials depends on the atomic interaction, microdefects (such as dislocation, grain boundary, crack etc.). Continuum mechanics has achieved a great success in the materials design, manufacture and other engineering applications, but due to the restriction of its basic postulates, there is an obvious drawback in the research of dislocation and grain boundary.

The advanced technology has made it possible to directly observe atomic configuration[1], which will provide many important experimental data. The embedded atom method has brought potential vigour to the research work on the atomic interaction. The N-body potential is a powerful tool for the study of the atomic interaction. Compared with the pair-potential model[2,3], it has a better physical foundation. The Cauchy's relation, $c_{12} = c_{44}$, which was deduced from the pair-potential is unrealistic. This drawback of the pair-potential can be naturally eliminated, if one introduces an embedded atom energy into the N-body potential. The N-body potential has a simple mathematical description and avoids the difficulty of multi-particle system quantum calculation.

2 A NEW N-BODY POTENTIAL

In the recent years, in order to study the physical property of materials, research workers proposed different N-body potentials and achieved many important results such as the dislocation emission[4], the grain boundary migration, the grain boundary segregation and breaking[5], the interaction of grain boundary and dislocation[6].

Received 1 July 1995, revised 25 August 1996
* The project supported by the National Natural Science Foundation of China

According to the EAM[7] method, the total energy E_T of an assembly of atoms at position r_i is

$$E_T = \frac{1}{2}\sum_{i,j,i\neq j}\phi(r_{ij}) + \sum_i F\left(\frac{\rho_i}{\rho_e}\right) \tag{1}$$

where r_{ij} is the distance between atoms i and j, $\phi(r_{ij})$ is the pair-potential, $F(\rho_i/\rho_e)$ is the embedding energy function.

Johnson[8,9] assumed that the electron density at any site normally is taken as a linear superposition of its neighbor atom electron density

$$\rho_i = \sum_{i,j\neq i}\rho_j^a\left(\frac{r_{1e}}{r_{ij}}\right) \tag{2}$$

ρ_j^a is assumed to have the form of a power term that is an approximation of Hartress-Fork's exponential expression. For a monoatom metal, ρ_j^a is

$$\rho_j^a = \left(\frac{r_{1e}}{r_{ij}}\right)^\beta \tag{3}$$

By combining the triaxial universal function with tight-binding theory and the concepts of G_{voigt} average shear modulus, Johnson[8,9] proposed the embedding function as follows

$$F\left(\frac{\rho}{\rho_e}\right) = F_0\left[\frac{n}{n-m}\left(\frac{\rho}{\rho_e}\right)^m - \frac{m}{n-m}\left(\frac{\rho}{\rho_e}\right)^m\right] \tag{4}$$

After a series of analyses, he concluded that for Mo metal $\beta = 5.029$ and $F(\rho/\rho_e)$ can be approximated by a straight line near $\rho = \rho_e$, ρ_e is the electron density at equilibrium, r_{1e}, r_{2e} are the first- and second neighbor atom distances respectively. The relations of the equilibrium equation, the elastic constants and the N-body potential are[8,9]

$$A_{kl} + F'(1)V_{kl} = 0 \tag{5}$$

$$A_{kl} = \frac{1}{2}\sum_i \rho_i a_k^i a_l^i/a^i \tag{6}$$

$$V_{kl} = \sum_i \rho_i a_k^i a_l^i/a^i \tag{7}$$

$$\phi_i' = \frac{d\phi(r_{ij})}{dr_{ij}} \tag{8}$$

$$C_{11} = [B_{11} + F'(1)W_{11} + F''(1)V_{11}^2]/\Omega_0 \tag{9}$$

$$C_{12} = [B_{12} + F'(1)W_{12} + F''(1)V_{11}^2]/\Omega_0 \tag{10}$$

$$C_{44} = [B_{12} + F'(1)W_{12}]/\Omega_0 \tag{11}$$

where C_{11}, C_{12}, C_{44} are the elastic constants, $B_{11}, B_{12}, W_{11}, W_{12}$ can be expressed by the N-body potential, a_k^i is the k^{th} component of the position vector to i^{th} neighbor. Ω_0 is the atom volume. Because Mo is a bcc crystal, in a cell, there is an atom in the center, eight atoms at the corner and 1/8 volume occupied by each atom. Altogether, there are two atoms $(1 + 8 \times 1/8 = 2)$ in a cell and a cell volume is a_0^3, so $\Omega_0 = 0.5a_0^3$.

$$B_{11} = \frac{1}{2}\sum_i(\phi_i'' - \phi_i'/a_i)a_1^i a_1^i a_1^i a_1^i/(a^i)^2 \tag{12}$$

$$B_{12} = \frac{1}{2}\sum_i (\phi_i'' - \phi_i'/a_i)a_1^i a_1^i a_2^i a_2^i/(a^i)^2 \tag{13}$$

$$W_{11} = \frac{1}{2}\sum_i (\rho_i'' - \rho_i'/a_i)a_1^i a_1^i a_1^i a_1^i/(a^i)^2 \tag{14}$$

$$W_{12} = \frac{1}{2}\sum_i (\rho_i'' - \rho_i'/a_i)a_1^i a_1^i a_2^i a_2^i/(a^i)^2 \tag{15}$$

Assuming

$$F'(1) = 0 \tag{16}$$

Equation (5) becomes

$$A_{kl} = 0 \tag{17}$$

The anisotropic ratio

$$A = \frac{C'}{C} \tag{18}$$

The Voigt average shear modulus

$$G_{\text{vogit}} = (3C + 2C')/5 \tag{19}$$

The vacancy formation energy

$$E_{IV}^F = \frac{1}{2}\phi_{ij}\mid_{\text{equilibrium}} \tag{20}$$

Here $C = C_{44}$, $C' = (C_{11} - C_{22})/2$. The pair potential proposed by Johnson[8,9] is

$$\phi\left(\frac{r_{ij}}{r_{1e}}\right) = B_0 + B_1\left(\frac{r_{ij}}{r_{1e}} - 1\right) + B_2\left(\frac{r_{ij}}{r_{1e}} - 1\right)^2 + B_3\left(\frac{r_{ij}}{r_{1e}} - 1\right)^3 \tag{21}$$

The coefficient B_i in (21) can be solved uniquely by Eqs. (17)~(20). Substituting (4) and (21) into (1), one can obtain Johnson's N-body potential.

The simulation results of the pair potential are in good agreement with the material mechanical behavior, if the material deformation is small. But as the material deformation is large , the calculation results given by the pair potential are remarkably deviated from the material mechanical behaviors. In order to eliminate the drawback of the pair potential (21), we think that the pair potential should not only satisfy Eqs. (17)~(21), but also satisfy the following continuous conditions.

$$\phi = 0 \quad \text{at} \quad r = r_c \tag{22}$$

$$\phi' = 0 \quad \text{at} \quad r = r_c \tag{23}$$

where r_c is the cutoff distance. Following Johnson's suggestion, $r_c = 1.25a_0$, where a_0 is the crystal constant, we propose the pair potential

$$\phi\left(\frac{r_{ij}}{r_{1e}}\right) = B_0 + B_1\left(\frac{r_{ij}}{r_{1e}} - 1\right) + B_2\left(\frac{r_{ij}}{r_{1e}} - 1\right)^2 + B_3\left(\frac{r_{ij}}{r_{1e}} - 1\right)^3 + H(r_{ij} - r_{2e})\left[B_4\left(\frac{r_{ij}}{r_{1e}} - 1\right)^3 + B_5\left(\frac{r_{ij}}{r_{1e}} - 1\right)^3\left(\frac{r_c}{r_{2e}} - 1\right)\right]\Big/\left(\frac{r_c}{r_{2e}} - 1\right)^3 \tag{24}$$

$H(r_{ij} - r_{2e})$ is a step function. B_i in (24) can be solved uniquely by above conditions. The results are

B_0	B_1	B_2	B_3	B_4	B_5
−1.65	11.58	−0.325	−0.45	−1.06	3.8

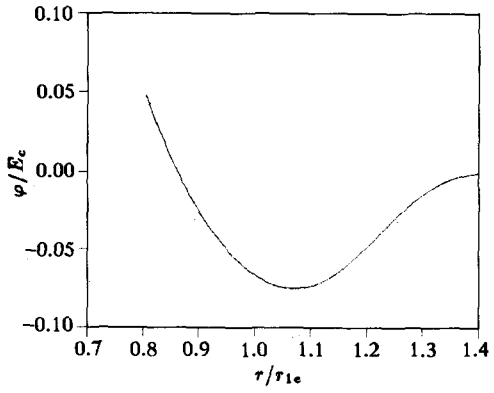

Fig.1 Scaled pair potential φ/E_C vs. scaled separation r/r_{1e}

Figure 1 is the pair potential, scaled energy ϕ/E_c against scaled separation r/r_{1e}. The binding energy $E_c = 6.81$(ev), the unit of $B_i(i = 0, \cdots, 5)$ is ev. The difference between potentials (24) and (21) is the last term of the Eq.(24) with a step function $H(r_{ij} - r_{2e})$. The embedding function (4) proposed by Johnson[9] is quite simple, but has no direct relevance to material mechanical behavior. We suggest that the embedding function should be closely related to the material mechanical behavior. A good embedding function should guarantee that the calculation predictions to be consistent with the mechanical response of the materials even at large deformation.

Based on the first principle, Rose and co-workers[10] proposed a triaxial universal function, Rice and co-workers[11] extended it to the uniaxial extension.

$$\sigma_{yy} = \sigma_{\max} \mathrm{e}^{\Delta y/L} \mathrm{e} \frac{\Delta y}{L} \tag{25}$$

$\sigma_{\max}$ and L can be determined by experiment, L is an analogue to Thomas-Fermi characteristic scale of screen distance in a metal. Δy is the relative displacement of two neighbor atomic plane along the loading direction. It is natural that we should apply the uniaxial universal formula (25) proposed by Rice and co-workers[11] to determine the embedding energy function. Hiroaki and Kurishn's[12] experiment of single crystal Mo indicated that when $\varepsilon_{yy} = 7.5\%$, the stress reaches the maximum. For the ideal single crystal Mo, $\sigma_{\max}$ should be equal to G/π, about 40 GPa and L is also defined. The internal stress produced by the N-body potential is given by the paper [13].

$$\sigma_{kl} = \Big[\sum_{i,j,i \neq j} \frac{1}{2} \phi' \Big(\frac{r_{ij}}{r_{1e}} \Big) + F' \Big(\frac{\rho_i}{\rho_e} \Big) \rho'_{i,j} \Big] \frac{r_{ij}^k r_{ij}^l}{r_{ij}} \tag{26}$$

The coordinate system is selected to be x, y and z axes along [100], [010], [001], respectively. The calculation is carried out under the uniaxial extension in specifying displacement. Along z direction, there are six layers and 100 atoms per x-y plane, the number of total atoms is 600. Under extension in y direction, all atoms experience the same relative displacement Δy per step, $\Delta y = 0.1 a_0$, a_0 is the crystal constant and there is not any displacement along x, z direction. Because single crystal Mo is of a periodicity along x, y, z direction, all atoms

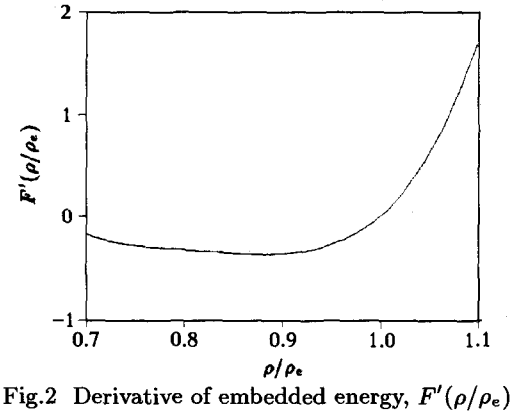

Fig.2 Derivative of embedded energy, $F'(\rho/\rho_e)$ vs. scaled electron density ρ/ρ_e

have the same environment. When the displacements of 600 atoms are specified, we can calculate the stress from Eqs. (25) and (26), substitute (24) into (26), have the stress from (26) to be the same as from (25), adjust the embedding energy and obtain the derivative of the embedding energy. Figure 2 shows that the derivative of the embedding energy plotted against the scaled electron density ρ/ρ_e, ρ_e is the electron density at equilibrium. The derivative of the embedding function $F'(\rho/\rho_e)$ can be expressed by the following fitting formula

$$F'\Big(\frac{\rho}{\rho_e}\Big) = \begin{cases} -10\sqrt{0.227^2 - \Big(\frac{\rho}{\rho_e} - 0.778\Big)^2} + 19 & 0.68 \le \frac{\rho}{\rho_e} \le 0.775 \\ -0.72\Big(\frac{\rho}{\rho_e} - 0.775\Big) - 0.3 & 0.775 \le \frac{\rho}{\rho_e} \le 0.83 \\ -10\sqrt{0.63^2 - \Big(\frac{\rho}{\rho_e} - 0.88\Big)^2} + 0.59 & 0.83 \le \frac{\rho}{\rho_e} \le 1.01 \end{cases} \tag{27}$$

Substituting (24) and the integration of (27) into (1), we can get a new N-body potential, the unit of (27) is ev.

3 EXAMINATION OF POTENTIAL

In order to examine the new N-body potential, the several different orientations of single crystals are calculated under extension and pure shear using molecular dynamics method and specified displacements procedure respectively.

3.1 Uniaxial Extension (Specified Displacement)

The coordinate system is selected to be x, y and z axes along [100], [010], [001], respectively. There are six layers of x-y atomic planes along z direction, 100 atoms per x-y plane, the number of total atoms is 600. Loading is the same as in the above section, there is a periodicity along x, y and z direction respectively. The displacements of 600 atoms are specified, the stress can be calculated from (26), the result is plotted in Fig. 3.

3.2 Uniaxial Extension (Molecular Dynamics Simulation)

The coordinate system is the same as the case of above specified displacement, x, y and z are along [100], [010], [001], respectively. There are two layers along z direction and the periodicity along x and z directions. Whole block is divided into the outer and inner regions, see Fig.4. The outer region is called boundary or loading region, the discrete atoms in the boundary region can be loaded by specified displacements. The atoms in the inner region follow the Newton's law.

$$F_i = -\frac{\partial E_T}{\partial r_i} = m_i v_i \tag{28}$$

The molecular dynamics simulation is carried out by the Leap-frog Algorithm as follows

$$v_i(t + \Delta t/2) = (1 - \eta)v_i(t - \Delta t) + \frac{F_i}{m_i}\Delta t \tag{29}$$

$$r_i(t + \Delta t) = r_i(t) + v_i(t + \Delta t/2)\Delta t \tag{30}$$

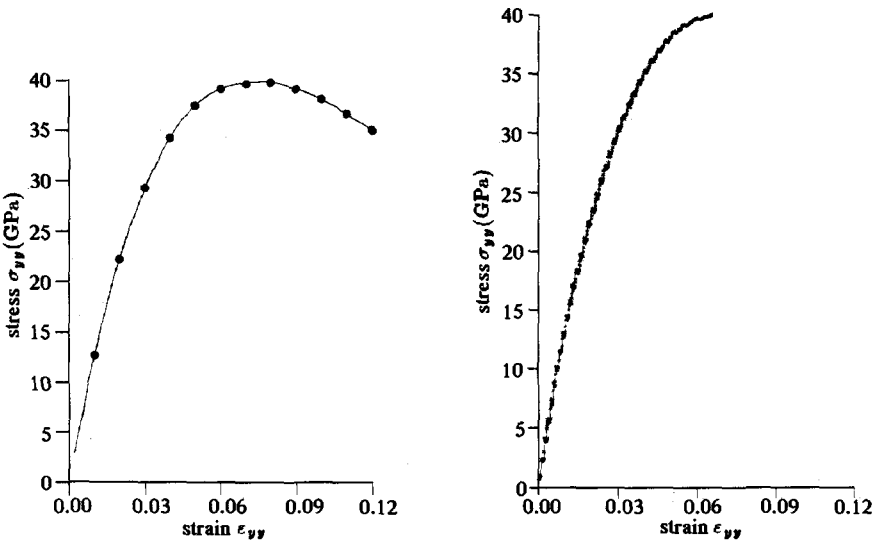

(a) specified displacement (b) molecular dynamics

Fig.3 Under simple extension, stress vs. strain

m_i, v_i is the mass and velocity of the i-th atom respectively. The loading strain rate is 0.001 19/ps, the time step is 1.256×10^{-14}s, η is the numerical damping parameter which is taken as 0.1 or 0 in the relaxation and loading respectively. Compared to Figs.3a and 3b the result is quite well.

3.3 Pure Shear (Specified Displacement)

The coordinate system is selected to be x, y and z axes along [110], [1$\bar{1}$0] and [001], respectively. The size and number of atoms is the same as that of specified displacement under extension. The displacements of all atoms are specified in pure shear strain, the stresses are calculated from (26) and the result is in Fig.5.

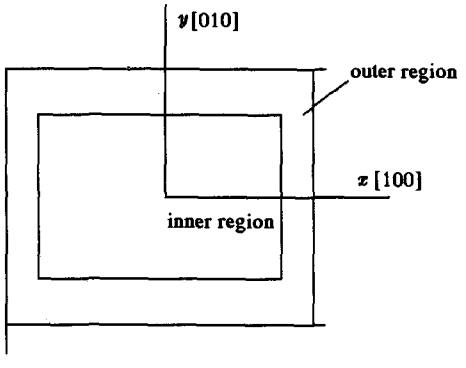

Fig.4 Schematic diagram for the simulated atom model

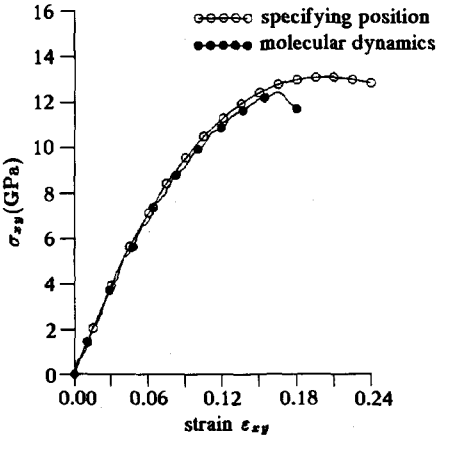

Fig.5 Pure shear (specified displacement and molecular dynamics), shear stress vs. shear strain

3.4 Pure Shear (Molecular Dynamics Simulation)

The coordinate system is the same as that of above case 3. Axes x, y and z are along [110], [1$\bar{1}$0], [001], respectively. Along z direction, there are two layers. The calculating method and loading rate is the same as the case of simple extension. Only the atom displacements in the boundary region are specified. From Fig.5 we can see that only the result in molecular dynamics is in good agreement with that in specified displacement. The curve of stress plotted against strain is of a slight wave in molecular dynamics. It is reasonable that atoms move continuously in the loading. When stress reaches 12 Gpa, along (110)/[1$\bar{1}$0] shear, the crystal lattice becomes unstable and the stress declines suddenly.

4 THE DISLOCATION EMISSION

4.1 The Atom Lattice Geometry

The parallelepiped with a slit is used as the simulated cell in the present calculation. The coordinate system is selected to be x, y and z axes along [111], [1$\bar{1}$0], [11$\bar{2}$], respectively. The periodicity along [111] is 3 layers, along [1$\bar{1}$0] is 2 layers and along [11$\bar{2}$] is 6 layers. The length of simulated cell along x-direction is $100 \times \frac{\sqrt{3}}{2}a_0$, along y-direction is $36 \times \frac{\sqrt{2}}{2}a_0$, along z-direction is $6 \times \frac{\sqrt{6}}{6}a_0$, the left side of boundary to crack tip is $30 \times \frac{\sqrt{3}}{2}a_0$. The separation of the upper and lower crack planes is taken to be $2\sqrt{2}a_0$. The number of atoms in the present simulation is about 10 830, see Fig.6.

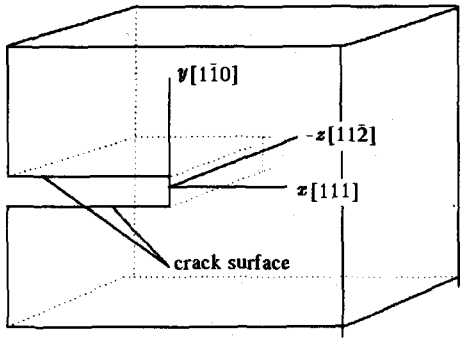

Fig.6 Schematic diagram for the simulated atom model

4.2 The Boundary Conditions

The boundary conditions applied to the discrete atom in the outer region is that of a prescribed displacement distribution dictated by mode II with K_2 field in x-y plane.

$$U_x = \frac{K_2}{4\mu}\sqrt{\frac{r}{2\pi}}[(2\kappa+3)\sin\theta/2 + \sin\theta/3]$$

$$U_y = \frac{K_2}{4\mu}\sqrt{\frac{r}{2\pi}}[(2\kappa+3)\cos\theta/2 + \cos\theta/3] \tag{31}$$

where $\kappa = 3 - 4\nu$,ν is the Poisson's ratio.

4.3 Result and Discussion

In the present calculation, the stress intensity factor K_2 is chosen as the loading parameter, loading rate is $\dot{K}_2 = 0.027\,85(\mathrm{MPam}^{1/2}/\mathrm{ps})$. Along z direction, six layers of atom planes are selected and the atoms in the inner region could move in z direction. From Fig.7, we found that when $K_2 = 1(\mathrm{MPam}^{1/2})$, a dislocation begins emission from the crack tip. Before the dislocation is emitted, the result of molecular dynamics is in good agreement with that of the elastic solution. From Fig.7 and Fig.9, we find that in bcc crystal Mo, a

perfect dislocation can be dissociated into 3 partial dislocations. But fcc crystal Cu is dissociated into 2 partial dislocations[14]. After the dislocation emission, see Fig.10, the stress distribution near crack tip given by MD is deviated from the K field but in good agreement with that of the K-b field[15] which takes into account of the contribution of the emitted dislocations:

$$\sigma_{xy} = \frac{K_2}{\sqrt{2\pi x}} + \sum_i \frac{G}{2\pi(1-\mu)} \sqrt{\frac{x_i}{x}} \frac{b}{x - x_i} \tag{32}$$

Since Eq.(32) is not suitable at the dislocation center, a modification by Peierls formula is introduced around the dislocation centers.

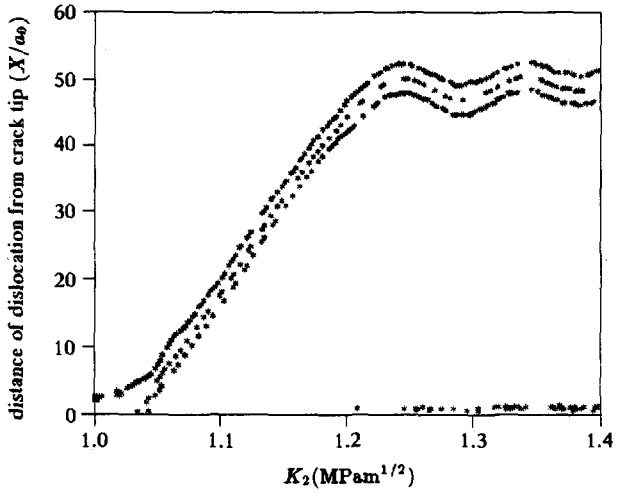

Fig.7 Distance of dislocation position from crack tip plotted against stress intensity

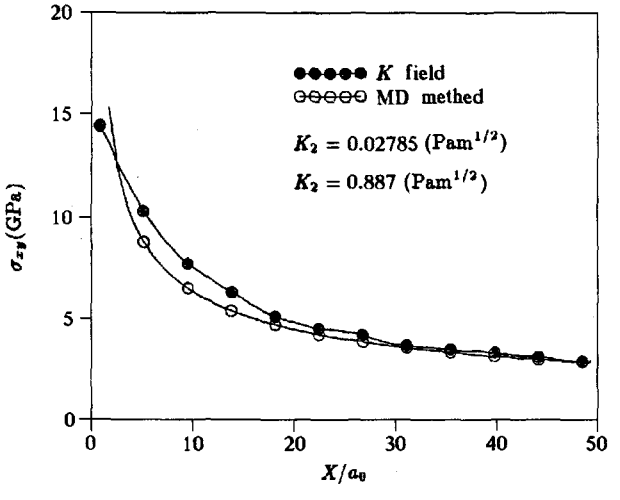

Fig.8 Before dislocation emitted from crack tip, the result of molecular dynamics compared to the elastic solution. The shear stress plotted against distance from crack tip.

$$\sigma_{xy} = \frac{Gb}{2\pi(1-\mu)} \frac{x}{x^2+\zeta^2} \tag{33}$$

where b, is the Burgers vector, ζ is the radius of dislocation core.

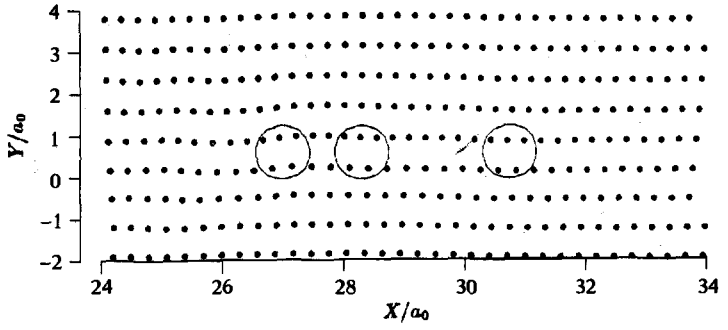

Fig.9 The atomic configure, plotted the position of dislocation

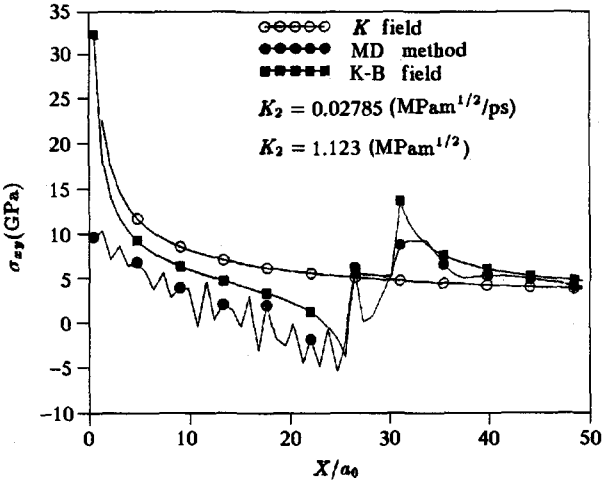

Fig.10 After dislocation emitted from crack tip, the result of (MD) compared to the elastic solution, K-b field. The shear stress plotted against distance from crack tip.

5 CONCLUSIONS

(1) This paper proposed a new N-body potential for metal Mo, the method can be applied to other metals.

(2) By examination of extension and pure shear loading, the calculation result of N-body potential is in good agreement with the mechanical behavior of the material.

(3) The new N-body potential proposed by this paper can be used to simulate the dislocation emission from the crack tip and the result is in good agreement with that of the elastic solution.

(4) The MD simulation shows that, in bcc crystal Mo, a perfect dislocation can be dissociated into 3 partial dislocations, but in fcc crystal Cu, a perfect dislocation can only be dissociated into 2 partial dislocations.

(5) The critical stress intensity factor at initiation of a dislocation emission from the crack tip for the bcc crystal Mo is about 3 times larger than that of fcc crystal Cu.

(6) It is obvious that the displacement boundary condition has effect on the nucleation of dislocation. When the leading dislocation is inhibited at boundary, it affects dislocation emission continuously.

REFERENCES

1 Berndt R, Gaisch R, Schneider WD. Atomic resolution in photon emission induced by scanning tunneling microscope. *Physical Review Letter*, 1995, 74(1): 102~105

2 Wang GJ, Sutton AP, Vitek V. A computer simulation study of [001] and [111] tilt boundaries: The multiplicity of structure. *Acta Metall*, 1984, 32(7): 1093~1104

3 Decelis B, Argon AS, Yip S. Molecular dynamics simulation of crack tip processes in alpha-iron and copper. *J Appl Phys*, 1983, 54(9): 4864~4878

4 Kitagawa H, Naktani A, Shibutani Y. Molecular dynamics study of crack initiation. In: Tokuda M, Xu B, Senoo M. Proceedings of IMMM'93 International Seminar Microstructures and Mechanical Properties of New Engineering Materials, Edited Mie University, Japan. Mie Academic Press, 1993. 19~26

5 Zhou FX, Peng BY, WU XJ. Molecular dynamics study of deformation and fracture for pure and bismuth-segregated tilt copper bicrystals. *J Appl Phys*, 1990, 68(2): 548~555

6 Zhang YW, Wang TC, Tang QH. Brittle and ductile fracture at the atomistic crack tip in copper crystals. *Script Metall Mater*, 1995, 33(2): 267~274

7 Daw MS, Baskes MI. Embedded-atom method: derivation and application to impurities, surface, and other defects in metals. *Phys Rev B*, 1984, 29(12): 6443~6453

8 Johnson RA. Analytic nearest-neighbor model for fcc metals. *Phys Rev B*, 1988, 37(8): 3924~3931

9 Johnson RA, Oh DJ. Analytic embedded atom method model for bcc metals. *J Mater Res*, 1989, 4(5): 1195~1201

10 Rose JH, Smith JR, Guinea F, Ferrante J. Universal features of the equation of state metals. *Phys Rev B*, 1984, 29(6): 2963~2969

11 Beltz GE, Rice JR. In: Lowe TC, Rollett AD, Follansbee PS, Daehn GS, eds. Modeling the Deformation of Crystalline Solids. The Minerals, Metals and Materials Society, 1991, 457~467

12 Kurishita H, Oishi A, Kubo H, Yoshinaga H. Grain boundary in molybdenum bicrystals with various [110] symmetric tilt boundaries. *Trans Japan Inst Metals*, 1985, 26(5): 341~352

13 Alber I, Bassani JL, et al. Grain boundaries as heterogeneous systems: atomic and continuum elastic properties. *Phil Trans R Soc Lond A*, 1992, 339: 555~586

14 Zhang YW, Wang TC, Tang QH. Molecular dynamics simulation of crack-tip processes in copper. *Acta Mechanica Sinica*, 1995, 11(1): 76~82

15 Ohr SM. Dislocation-crack interaction. *J Phys Chem Solids*, 1987, 48(11): 1007~1014